THE JOURNAL OF PHYSICAL CHEMISTRY B

Article

pubs.acs.org/JPCB

Arginine-Facilitated Isomerization: Radical-Induced Dissociation of Aliphatic Radical Cationic Glycylarginyl(iso)leucine Tripeptides

Qiang Hao,[†,‡,§] Tao Song,[†,§] Dominic C. M. Ng,[†,§] Quan Quan,[†] Chi-Kit Siu,[‡,*] and Ivan K. Chu*[,†]

[†]Department of Chemistry, The University of Hong Kong, Hong Kong, China

[‡]Department of Biology and Chemistry, City University of Hong Kong, Hong Kong, China

Supporting Information

ABSTRACT: The gas phase fragmentations of aliphatic radical cationic glycylglycyl(iso)leucine tripeptides ([G$^{\bullet}$G(L/I)]$^{+}$), with well-defined initial locations of the radical centers at their N-terminal α-carbon atoms, are significantly different from those of their basic glycylarginyl(iso)leucine ([G$^{\bullet}$R(L/I)]$^{+}$) counterparts; the former lead predominantly to $[b_2 - H]^{\bullet+}$ fragment ions, whereas the latter result in the formation of characteristic product ions via the losses of $^{\bullet}CH(CH_3)_2$ from [G$^{\bullet}$RL]$^{+}$ and $^{\bullet}CH_2CH_3$ from [G$^{\bullet}$RI]$^{+}$ through C_β–C_γ side-chain cleavages of the (iso)leucine residues, making these two peptides distinguishable. The α-carbon-centered radical at the leucine residue is the key intermediate that triggers the subsequent C_β–C_γ bond cleavage, as supported by the absence of $^{\bullet}CH(CH_3)_2$ loss from the collision-induced dissociation of $[G^{\bullet}RL_{\alpha\text{-Me}}]^{+}$, a radical cation for which the α-hydrogen atom of the leucine residue had been substituted by a methyl group. Density functional theory calculations at the B3LYP 6-31++G(d,p) level of theory supported the notion that the highly basic arginine residue could not only increase the energy barriers against charge-induced dissociation pathways but also decrease the energy barriers against hydrogen atom transfers in the GR(L/I) radical cations by ~10 kcal mol^{-1}, thereby allowing the intermediate precursors containing α- and γ-carbon-centered radicals at the (iso)leucine residues to be formed more readily prior to promoting subsequent C_β–C_γ and C_α–C_β bond cleavages. The hydrogen atom transfer barriers for the α- and γ-carbon-centered GR(L/I) radical cations (roughly in the range 29–34 kcal mol^{-1}) are comparable with those of the competitive side-chain cleavage processes. The transition structures for the elimination of $^{\bullet}CH(CH_3)_2$ and $^{\bullet}CH_2CH_3$ from the (iso)leucine side chains possess similar structures, but slightly different dissociation barriers of 31.9 and 34.0 kcal mol^{-1}, respectively; the energy barriers for the elimination of the alkenes $CH_2{=}CH(CH_3)_2$ and $CH_3CH{=}CHCH_3$ through C_α–C_β bond cleavages of γ-carbon-centered radicals at the (iso)leucine side chains are 29.1 and 32.8 kcal mol^{-1}, respectively.

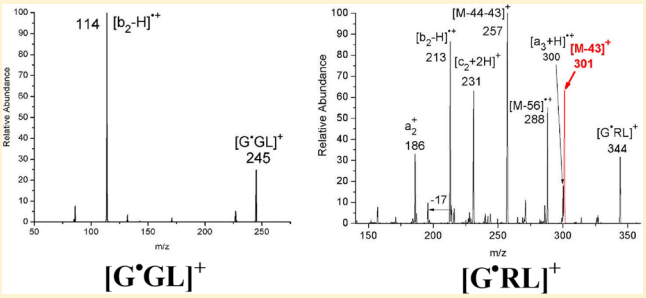

INTRODUCTION

Shotgun proteomics uses mass spectrometry techniques to identify proteins on the basis of information obtained from the gas phase fragmentation of the protonated forms of their constituent peptides via bond cleavages along the peptide backbone, promoted through collision-induced dissociation (CID) under low-energy conditions.[1] Correct assignment of the resulting peptide fragment ions relies on the ability to unambiguously distinguish the constituent amino acid residues in terms of differences in their masses. Although isomeric/isobaric amino acids, such as leucine and isoleucine, are not readily differentiable in terms of their masses alone, they can be identified using complementary information obtained from the dissociations of odd-electron peptide radical cations, which produce fragment ions through side-chain bond cleavages.[2−6]

Several techniques have been developed recently to generate different types of peptide radical cations, including hydrogen-rich radical cations,[2−5] $[M + nH]^{\bullet(n-1)+}$, and molecular peptide radical cations, $M^{\bullet+}$.[7−17] Fragmentations of these radical cations with aliphatic, aromatic, and basic amino acid residues have been explored recently through MS/MS experiments and density functional theory (DFT) calculations.[18−43] Unlike the dissociations of protonated peptides that are dominated by charge-directed amide bond cleavages and form b_n^{+}/y_n^{+} ion pairs via the mobile-proton mechanism,[44−47] the fragmentation behavior of peptide radical cations is dictated not only by the location of the charge but also by the site and mobility of the radical. These two factors are competitive.[13] For example, sequestering the proton onto a basic amino acid residue significantly reduces the efficiency of charge-directed fragmentations, but enhances that of radical-driven charge-remote pathways. Some commonly observed radical-driven pathways include the formation of a_n^{+} ions and $[c_n + 2H]^{+}/[z_n - H]^{\bullet+}$ ion pairs, both originating from β-carbon-centered radical intermediates,[41,43] and side chain losses from nonaromatic

Received: February 26, 2012
Revised: June 6, 2012
Published: June 6, 2012

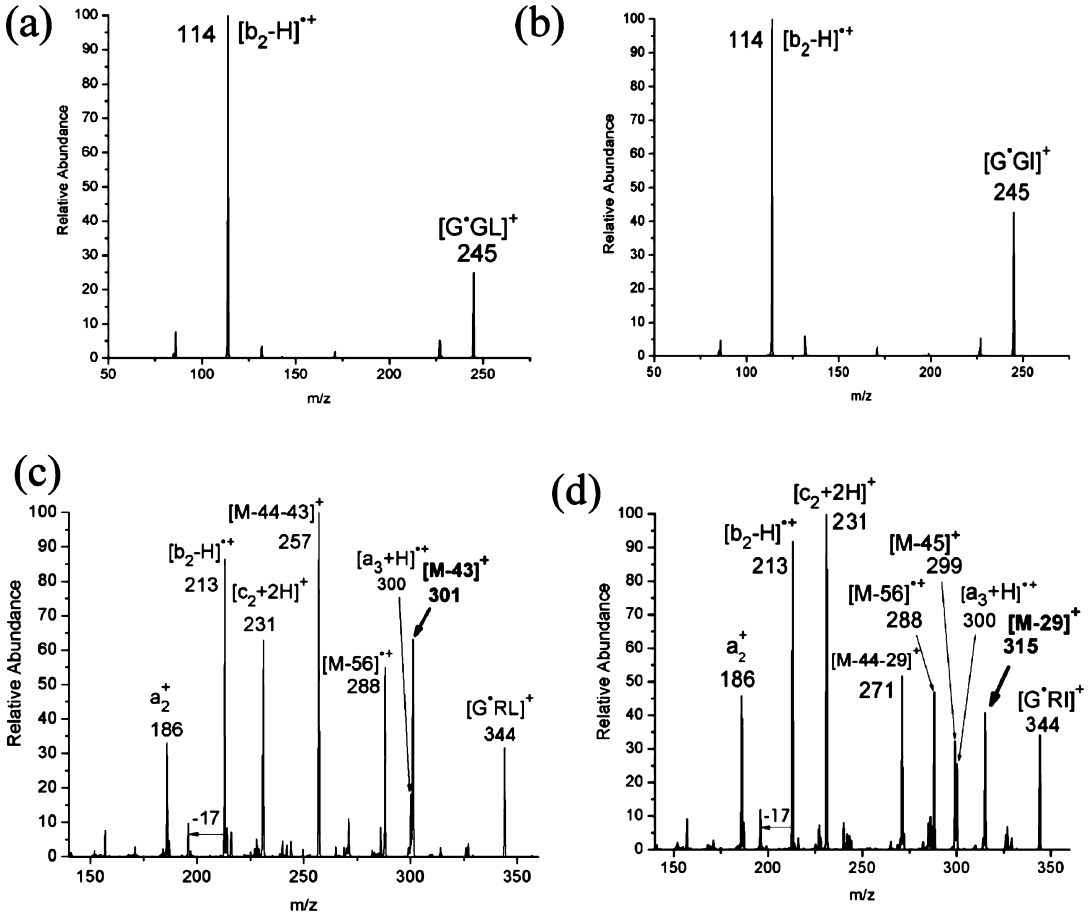

Figure 1. CID spectra, with unit mass resolution, of (a) $[G^{\bullet}GL]^+$, (b) $[G^{\bullet}GI]^+$, (d) $[G^{\bullet}RL]^+$, and $[G^{\bullet}RI]^+$. The amplitudes of the resonance excitation RF voltage for $[G^{\bullet}GL]^+$, $[G^{\bullet}GI]^+$, $[G^{\bullet}RL]^+$, and $[G^{\bullet}RI]^+$ were 0.62, 0.59, 0.97, and 0.97 eV, respectively.

residues, including isomeric (iso)leucine residues, arising from α- or γ-centered radical intermediates.[16,25,43,48−50]

Radical migrations along a peptide backbone are usually hindered by substantial energy barriers, with the radical being "trapped" on the α-carbon atoms through captodative radical stabilization resulting from the presence of vicinal electron-donating amino or amido nitrogen atoms and electron-withdrawing carbonyl groups.[51,52] Recent CID and DFT studies for the simplest tripeptide radical cations, those of glycylglycylglycine (GGG), suggested that the energy barriers for the radical migrations are significantly higher than those for dissociations, resulting in very distinct CID spectra for the three GGG tautomers with the radical initially generated on the α-carbon atom of a different glycine residue ($[G^{\bullet}GG]^+$, $[GG^{\bullet}G]^+$, and $[GGG^{\bullet}]^+$; hereafter, $X^{\bullet}$ denotes the radical being located on the α-carbon of an amino acid (X) residue).[51,53,54] A similar study for glycylglycyltryptophan (GGW) also found that its radical cations with the initial radical site located on the α-carbon atom ($[G^{\bullet}GW]^+$) or the indolyl ring ($[GGW]^{\bullet+}$) are not interconvertible on the time scale of the experiments, again due to the presence of high energy barriers against these radical migrations.[52] These barriers are greatly reduced in the presence of a highly basic arginine residue. For example, the CID spectra of $[G^{\bullet}RW]^+$ and $[GRW]^{\bullet+}$ are almost identical because the radical becomes freely migratable.[54] Thus, the radical mobility is greatly influenced by the nature of the charge carriers.[51,55,56]

In this study, we investigated the influence of the arginine residue on the radical migrations and fragmentations of (iso)leucine-containing peptide radical cations. Direct evidence, obtained from CID experiments for model tripeptide radical cations (glycylglycyl(iso)leucine $[G^{\bullet}G(L/I)]^+$ and glycylarginyl(iso)leucine $[G^{\bullet}R(L/I)]^+$, with the radicals initially generated at the N-terminal α-carbon atom, and their derivatives), revealed that migration of the radical to the α-carbon atom of the (iso)leucine residue is a prerequisite for its subsequent $C_\beta-C_\gamma$ bond cleavage. We also used DFT calculations to examine the mechanistic role of the γ-carbon-centered radical on the $C_\alpha-C_\beta$ bond cleavages of the (iso)leucine residues.

EXPERIMENTAL SECTION

Materials. All chemicals were obtained commercially (Aldrich and Sigma, St Louis, MO; Bachem, King of Prussia, PA). The Cu(II)(terpy)$(NO_3)_2$ (terpy: 2,2′:6′,2″-terpyridine) and [Co(III)(salen)]Cl [salen: *N*,*N*′-ethylenebis-(salicylideneaminato)] complexes[57,58] and the tripeptides[59] were synthesized according to procedures described in the literature.

Mass Spectrometry. All mass spectrometry experiments were conducted using a quadrupole ion trap instrument (Finnigan LCQ, ThermoFinnigan, San Jose, CA, USA). Samples, typically consisting of 600 μM of a metal complex and 50 μM of a tripeptide in a H_2O/MeOH (1:1) solution, were delivered for electrospraying (flow rate: 30 μL h^{-1}) by a syringe pump (Cole Parmer, Vernon Hills, IL). CID spectra were acquired using He as the collision gas, with injection and

dx.doi.org/10.1021/jp301882p | J. Phys. Chem. B 2012, 116, 7627−7634

excitation times of 200 and 50 ms, respectively. The amplitude of the excitation was optimized for each experiment. The α-carbon-centered radical cations ($[G^{\bullet}G(L/I)]^+$, $[G^{\bullet}R(L/I)]^+$, and $[G^{\bullet}RL_{\alpha\text{-Me}}]^+$, where $L_{\alpha\text{-Me}}$ denotes an α-methylleucine residue) were generated through neutral *p*-quinomethide losses from their respective tyrosine-terminated radical cations $[M]^{\bullet+}$ [M = YG(L/I), YR(L/I), and $YRL_{\alpha\text{-Me}}$], produced through CID of precursor $[Cu(II)(terpy)(M)]^{\bullet 2+}$ or $[Co(III)(salen)(M)]^+$ complexes.[51,52,54]

Computational Methods. Initial structural samplings were performed through Monte Carlo conformational searches at the PM3 semiempirical level using the Spartan program.[60] The resulting low-lying conformers were then optimized in the framework of DFT at the unrestricted B3LYP level[61] performed with the Gaussian 03 package.[62] Atomic orbitals were described by a Pople-type double-ζ 6-31++G(d,p) basis set, which includes polarization functions and a diffuse function for all atoms.[63,64] Stationary points on the potential energy surface (PES) of the isomerization and dissociation pathways were also optimized at this level of theory. Harmonic vibrational frequencies of all optimized structures were calculated to confirm that the structures were at local minima with all-real frequencies or at transition states with only one imaginary frequency. The local minima associated with each transition structure were verified using the intrinsic reaction coordinates method. Relative enthalpies at 0 K (ΔH_0°) and free energies at 298 K (ΔG_{298}°) were calculated from the electronic energies and the zero-point vibrational energies, the thermal energies, and the entropies obtained within the harmonic approximation.

RESULTS AND DISCUSSION

CID of $[G^{\bullet}GL]^+$, $[G^{\bullet}GI]^+$, $[G^{\bullet}RL]^+$, and $[G^{\bullet}RI]^+$. As in the case after the CID of $[G^{\bullet}GG]^+$,[51] dissociation of $[G^{\bullet}GL]^+$ and $[G^{\bullet}GI]^+$ produced predominantly the $[b_2 - H]^{\bullet+}$ radical cation at *m*/*z* 114 (Figures 1a and 1b, respectively). We observed a dramatic change in the fragmentation pattern when the glycine residue in the middle was replaced by an arginine residue to give $[G^{\bullet}RL]^+$ and $[G^{\bullet}RI]^+$ (Figures 1c and 1d, respectively), the CID of which produced additional fragment ions, including backbone-cleaved fragment ions (namely, $[b_2 - H]^{\bullet+}$, a_2^+, $[a_3 + H]^{\bullet+}$, and $[c_2 + 2H]^+$), as well as $[M - 56]^{\bullet+}$ ions produced through C_α–C_β bond cleavages of the leucine or isoleucine side chains. This phenomenon was probably due to the highly basic arginine residue sequestering the mobile proton and, thereby, making radical-driven fragmentations more favorable, both energetically[65] and kinetically.[52]

More importantly, the CID spectra of the two different tripeptide radical cations $[G^{\bullet}RL]^+$ and $[G^{\bullet}RI]^+$ were almost identical, except for some characteristic ions associated with losses of diagnostic neutral alkyl radicals—$^{\bullet}CH(CH_3)_2$ (43 Da) or $^{\bullet}CH_2CH_3$ (29 Da)—via side-chain C_β–C_γ bond cleavages of the leucine or isoleucine residue, respectively; they include $[M - 43]^+$ or $[M - 29]^+$, produced from the in situ side chain loss of $[G^{\bullet}RL]^+$ or $[G^{\bullet}RI]^+$, respectively, and $[M - 44 - 43]^+$ or $[M - 44 - 29]^+$, generated through sequential CO_2 and side chain losses. This phenomenon allows the leucine and isoleucine residues to be distinguished unambiguously.[25,28,43,66]

Notably, the $[M - 44 - 43]^+$ ion is isobaric with $[M - 87]^{\bullet+}$, which could be produced through neutral loss from the arginine side chain through C_β–C_γ cleavage. Because we did not observe the corresponding $[M - 87]^{\bullet+}$ species in the spectrum of $[G^{\bullet}RI]^+$, it is likely that the ion at *m*/*z* 257 resulted from the successive loss of the side chain of leucine from $[a_3 + H]^{\bullet+}$, in agreement with the literature.[25,43]

The formation of these characteristic product ions associated with the loss of $^{\bullet}CH(CH_3)_2$ or $^{\bullet}CH_2CH_3$ from $[G^{\bullet}R(L/I)]^+$, but not from $[G^{\bullet}G(L/I)]^+$, seems surprising at first glance because both radical cations share similar features, including the same C-terminal leucine or isoleucine residue and the same initial radical site at the N-terminal α-carbon atom. Similar side chain losses (i.e., $[a_3 + H]^{\bullet+}$) have been observed from the analogous systems $[GG(L/I) - CO_2]^{\bullet+}$, with their initial radical sites located at the C-terminal α-carbon atoms, produced directly through CID of the ternary metal complexes.[67] Thus, the occurrence of C_β–C_γ bond cleavage of the (iso)leucine residues from the $[G^{\bullet}G(L/I)]^+$ radical cations is largely determined by the ability to migrate the N-terminal α-radical to the C-terminal α-carbon atom. Such α-radical migrations can be facilitated by the presence of a basic arginine residue, which can sequester the mobile proton and, hence, increase the barriers against the charge-induced dissociation pathways while, on the other hand, decreasing the energy required to disrupt the hydrogen bonds during the course of radical migrations.[52,54] We would anticipate that the replacement of the middle glycine residue in $[G^{\bullet}G(L/I)]^+$ with an arginine residue to give $[G^{\bullet}R(L/I)]^+$ would lead to lower energy barriers against the radical migrations.

To elucidate the mechanism of the α-centered-radical-induced C_β–C_γ bond cleavages of the (iso)leucine side chains, we blocked the formation of the prerequisite α-carbon-centered radical at the C-terminal leucine residue by replacing it with an α-methyl leucine residue ($L_{\alpha\text{-Me}}$). A signal for the $[M - 43]^+$ ion was not evident after CID of $[G^{\bullet}RL_{\alpha\text{-Me}}]^+$ (Figure 2).

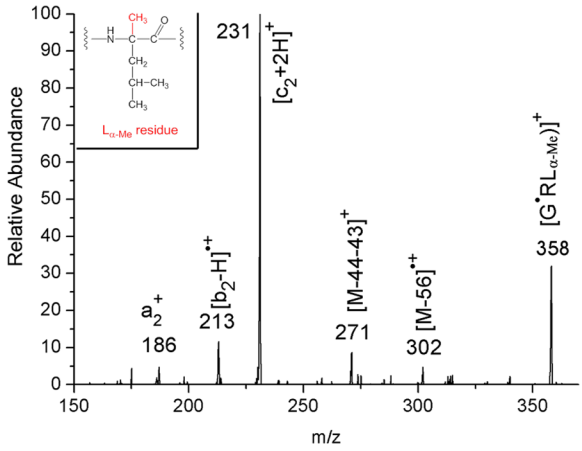

Figure 2. CID spectrum, with unit mass resolution, of $[G^{\bullet}RL_{\alpha\text{-Me}}]^+$. The amplitude of the resonance excitation RF voltage was 0.99 eV.

Following these experimental observations, we used DFT calculations to explore the PES of $[G^{\bullet}RL]^+$, with particular focus on how the N-terminal α-radical propagate to the prerequisite α-carbon atom of the (iso)leucine residue to trigger its distinctive side chain cleavage. We compared their energetics with those of nonarginine-containing analogs. In addition, we also examined the mechanisms behind the formation of the quite-abundant charge-related $[b_2 - H]^{\bullet+}$ ion.

Low-Energy Structures of GRL Radical Cations. Figure 3 displays the lowest-energy structures for different tautomers of the GRL radical cations. They are distonic ions, having the charge located on the guanidino group of the arginine residue

dx.doi.org/10.1021/jp301882p | J. Phys. Chem. B 2012, 116, 7627–7634

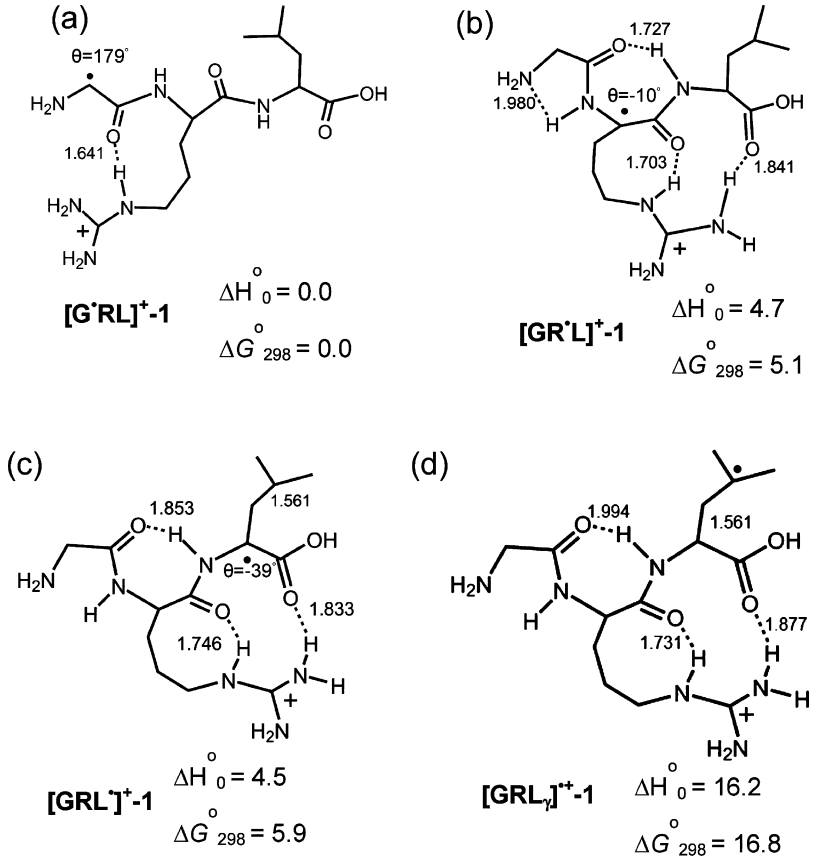

Figure 3. Optimized lowest-energy structures for (a) $[G^{\bullet}RL]^{+}$-1, (b) $[GR^{\bullet}L]^{+}$-1, (c) $[GRL^{\bullet}]^{+}$-1 and (d) $[GRL_{\gamma}^{\bullet}]^{+}$-1 (energies, kcal mol^{-1}; bond lengths, Å). The dihedral angles of H(C)−N−C_{α}−C for α-carbon radicals are also shown.

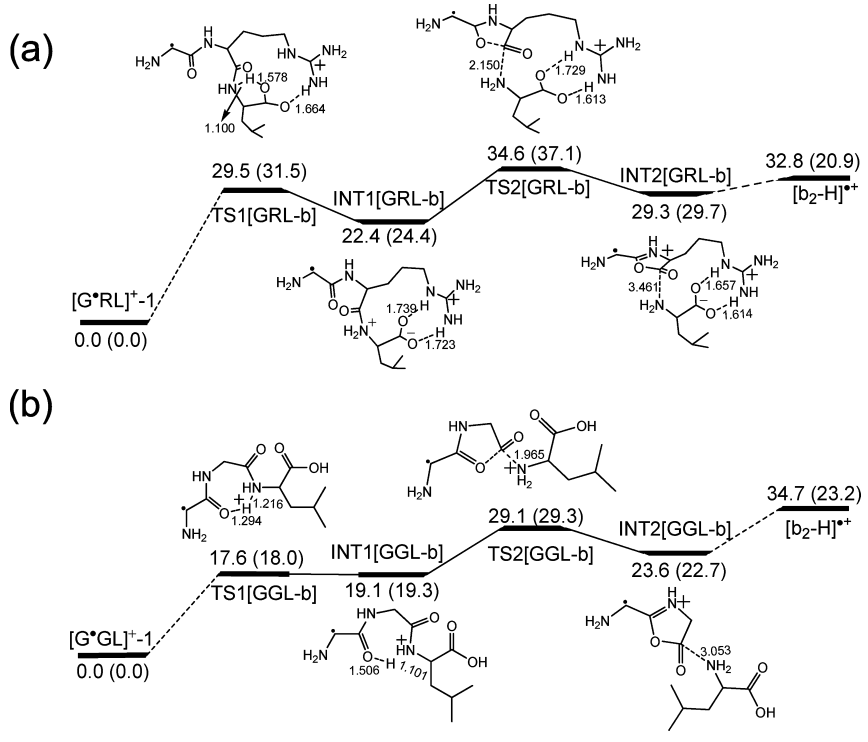

Figure 4. PES for the formation of $[b_2 - H]^{\bullet+}$ ion for (a) $[G^{\bullet}RL]^{+}$ and (b) $[G^{\bullet}GL]^{+}$ cases. The enthalpies at 0 K and free energies at 298 K (in parentheses) are shown in kcal mol^{-1}. Selected bond lengths are in Å.

and the radical located at (a) the N-terminal α-carbon atom ($[G^{\bullet}RL]^{+}$-1), (b) the middle α-carbon atom ($[GR^{\bullet}L]^{+}$-1), (c) the C-terminal α-carbon atom ($[GRL^{\bullet}]^{+}$-1), and (d) the γ-carbon atom of the leucine side chain ($[GRL_{\gamma}^{\bullet}]^{+}$-1). The α-

dx.doi.org/10.1021/jp301882p | J. Phys. Chem. B 2012, 116, 7627−7634

Table 1. Energy Barriers (enthalpies at 0 K, in kcal mol^{-1}) for the Radical Migrations among α-Carbon-Centered Tripeptide Radical Cations

	TS([G$^{\bullet}$XZ]$^{+}$-1 → [GX$^{\bullet}$Z]$^{+}$-1)			TS([GX$^{\bullet}$Z]$^{+}$-1 → [GXZ$^{\bullet}$]$^{+}$-1)			TS([G$^{\bullet}$XZ]$^{+}$-1 → [GXZ$^{\bullet}$]$^{+}$-1)		
	X = G	X = R	Δ	X = G	X = R	Δ	X = G	X = R	Δ
GGX[a]	44.7	36.2	8.5	49.2	39.7	9.5	62.3	48.2	14.1
GXW[b]	41.8	35.6	6.2	41.1	35.7	5.4	54.6	49.8	4.8
GXL	44.2	36.1	8.1	45.9	39.0	6.9	63.7	53.0	10.7
GXI	43.9	36.7	7.2	45.7	37.7	8.0	61.4	51.8	9.6

[a]References 51 and 73. [b]References 52 and 54.

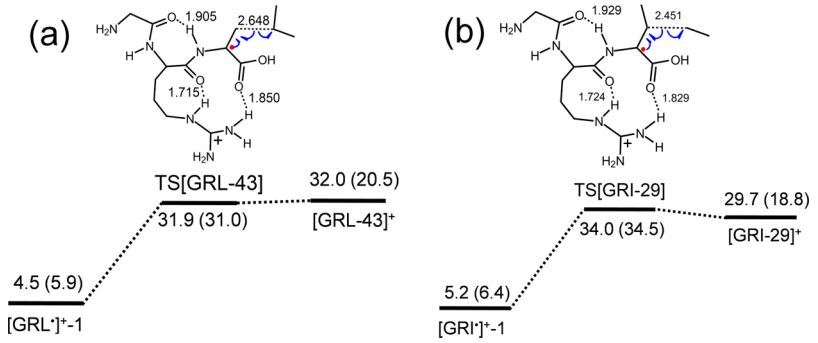

Figure 5. PES for the side cleavage of (a) [G$^{\bullet}$RL]$^{+}$ (43 loss) and (b) [G$^{\bullet}$RI]$^{+}$ (29 loss). The radicals as shown in the transition structures indicate their original location in the corresponding reactants. The enthalpies at 0 K and free energies at 298 K (in parentheses) are shown in kcal mol^{-1}. Selected bond lengths are in Å.

radicals in [G$^{\bullet}$RL]$^{+}$-1, [GR$^{\bullet}$L]$^{+}$-1, and [GRL$^{\bullet}$]$^{+}$-1 are stabilized captodatively by the electron-donating nitrogen atom of the amino or amido group and the electron-withdrawing carbonyl group of the amido or carboxylic group.

The electron-withdrawing effect can be further enhanced by the hydrogen bonds formed between the protonated guanidino group and the carbonyl oxygen atoms. The captodative effects in [GR$^{\bullet}$L]$^{+}$-1 and [GRL$^{\bullet}$]$^{+}$-1 are weaker than that in [G$^{\bullet}$RL]$^{+}$-1, due to (i) the electron-donating power of the −C(O)NH− groups being less effective than that of the N-terminal amino group and (ii) the hydrogen bonds formed between the guanidino group and the backbone carbonyl oxygen atoms, which impose geometric constraints, causing distortion of the planarity for the π-conjugation of the radical (the dihedral angle of the radical-containing H−N−C_{α}−C unit for [G$^{\bullet}$RL]$^{+}$-1 was 1°, compared with −10 and −39° for [GR$^{\bullet}$L]$^{+}$-1 and [GRL$^{\bullet}$]$^{+}$-1, respectively, making their energies higher than that of the lowest-lying [G$^{\bullet}$RL]$^{+}$-1 by 4.7 and 4.5 kcal mol^{-1}, respectively). The lowest-energy conformer of the γ-carbon-centered radical structure [GRL$_{\gamma}^{\bullet}$]$^{+}$-1 was similar to that of [GRL$^{\bullet}$]$^{+}$-1, except for the absence of the captodative radical stabilization in the former, resulting in its energy being 11.7 kcal mol^{-1} higher than that of [GRL$^{\bullet}$]$^{+}$-1 (or 16.2 kcal mol^{-1} higher than the global minimum structure [G$^{\bullet}$RL]$^{+}$-1). Because of the structural resemblance of GRL and GRI peptide radical cations, the relative energies of the tautomers of these two systems were also similar: the relative energies for the GRI peptide radical cations were 0.0 ([G$^{\bullet}$RI]$^{+}$-1), 5.3 ([GR$^{\bullet}$I]$^{+}$-1), 5.2 ([GRI$^{\bullet}$]$^{+}$-1), and 18.7 kcal mol^{-1} ([GRI$_{\gamma}^{\bullet}$]$^{+}$-1) (Supporting Information Figure S1).

Mechanisms for the Formation of [b_2 − H]$^{\bullet+}$ Ions. The formation of [b_2 − H]$^{\bullet+}$ species from a tripeptide radical cation has been suggested to proceed via a charge-directed pathway,[51,52,54] with a mechanism similar to the formation of b_2 ions from protonated peptides.[68−72] We examined the PES for this process using [G$^{\bullet}$RL]$^{+}$ and [G$^{\bullet}$GL]$^{+}$ as examples (Figure 4). A proton is first liberated from the carboxylic group at the C-terminus (for GRL) or backbone (for GGL) to bond with the nitrogen atom of the C-terminal amide group, forming intermediates INT1[GRL-b] or INT1[GGL-b]. The carbon atom of this protonated amide group then undergoes nucleophilic attack by the N-terminal amide oxygen atom, leading to an oxazolone intermediate (INT2[GRL-b] or INT2[GGL-b]), with barriers for [G$^{\bullet}$RL]$^{+}$ and [G$^{\bullet}$RI]$^{+}$ (34.6 and 35.2 kcal mol^{-1}, respectively) that are higher than those for [G$^{\bullet}$GL]$^{+}$ and [G$^{\bullet}$GI]$^{+}$ (both 29.1 kcal mol^{-1}). We also examined a salt-bridge anhydride pathway, as proposed for protonated arginine-containing peptides;[71,72] it had a high energy barrier of 44.0 kcal mol^{-1} (Supporting Information Scheme S1). Interestingly, the C−N bond cleavages are characterized by negative activation entropies; thus, the formation of [b_2 − H]$^{\bullet+}$ ions from [G$^{\bullet}$RL]$^{+}$ is kinetically hindered relative to that of its nonbasic-residue-containing analogue, [G$^{\bullet}$GL]$^{+}$.[52]

Mechanisms for the Formation of α-Carbon-Centered Radicals at the (Iso)Leucine Residues and the Respective 43 and 29 Da Losses through C_{β}−C_{γ} Bond Cleavages. Similar to the GRW cases,[54] the presence of the arginine residue in the GR(L/I) systems might also considerably lower the energy barriers of the radical migration pathways and favor the formation of radical-driven product ions. The CID of [G$^{\bullet}$R$L_{\alpha\text{-Me}}$]$^{+}$ (Figure 2) suggests that migration of the N-terminal α-radical of [G$^{\bullet}$R(L/I)]$^{+}$ to the α-carbon atom of the (iso)leucine residue, forming [GR(L/I)$^{\bullet}$]$^{+}$, is a prelude to subsequent C_{β}−C_{γ} bond dissociation. These radical migrations could propagate via either a series of stepwise 1,4-hydrogen-atom transfer from the first to the second and then to the third α-carbon atom or a direct 1,7-hydrogen-atom transfer from the first to the third α-carbon atom. Table 1 summarizes the energy barriers against such α-radical

dx.doi.org/10.1021/jp301882p | J. Phys. Chem. B 2012, 116, 7627−7634

migrations for the GR(L/I) and GG(L/I) systems (Figures S2 and S3 of the Supporting Information) and for the analogous GGG/GGR[51] and GGW/GRW[52,54] systems.

Our calculations suggested that, in general, the radical migration proceeds preferentially in a stepwise manner: the energy barriers for the stepwise 1,4-hydrogen-atom transfer mechanisms of the nonarginine-containing and arginine-containing peptides (41−49 and 35−40 kcal mol^{-1}, respectively) were 13−18 and 9−14 kcal mol^{-1} lower, respectively, than those for the direct 1,7-hydrogen-atom transfer mechanism. Among the 1,4-hydrogen-atom transfer barriers, those for the arginine-containing peptides were 5−10 kcal mol^{-1} (denoted as Δ in Table 1; average value, 7.5 kcal mol^{-1}; standard deviation, 1.3 kcal mol^{-1}) lower than those for the nonarginine-containing counterparts. We observed a similar effect among the 1,7-hydrogen-atom transfer barriers (a difference of 5−14 kcal mol^{-1}; average value, 9.8 kcal mol^{-1}; standard deviation, 3.8 kcal mol^{-1}). In general, the arginine residue tightly sequesters the proton, thereby facilitating radical migration along the backbone.[52,54,73]

The transition structures associated with the subsequent C_β−C_γ bond cleavages (denoted TS[GRL-43] and TS[GRI-29] in Figure 5) are similar to the respective local minimal structures $[GR(L^\bullet/I^\bullet)]^+$-1. The barriers against the bond cleavages in $[GRL^\bullet]^+$ and $[GRI^\bullet]^+$ are 27.4 and 28.8 kcal mol^{-1}, respectively (or 31.9 and 34.0 kcal mol^{-1}, respectively, relative to the lowest-energy isomers, $[G^\bullet RL]^+$-1 and $[G^\bullet RI]^+$-1, respectively). This barrier for GRL is slightly lower than that for GRI, presumably because a more stable secondary isopropyl radical is formed in the case of GRL and because the leucine side chain (431 Å^3) is larger than the isoleucine side chain (384 Å^3). (The sizes were defined as the volume within a contour of 0.001 electrons/Bohr^3 density.) The latter steric effect is also reflected in a slightly lengthened C_β−C_γ bond of 1.561 Å in $[GRL^\bullet]^+$-1 (Figure 3c), compared with that of 1.553 Å in $[GRI^\bullet]^+$-1 (Figure S1c of the Supporting Information). The overall dissociation processes, forming $[GRL - 43]^+$ and $[GRI - 29]^+$, are endothermic by 32.0 and 29.7 kcal mol^{-1}, respectively.

More specifically, the rate-determining steps for the C_β−C_γ bond cleavages of $[G^\bullet RL]^+$ and $[G^\bullet RI]^+$ are the radical migrations, with barriers of 39.0 and 37.7 kcal mol^{-1}, respectively, that are higher than those (34.6 and 35.2 kcal mol^{-1}, respectively) for the formation of their $[b_2 - H]^{\bullet+}$ radical cations. These results are consistent with our experimental observations that the abundances of $[b_2 - H]^{\bullet+}$ ions were generally higher than the abundances of the ions resulting from side chain losses (Figure 1). In addition, we did not observe signals for C_β−C_γ bond cleavages after the CID of $[G^\bullet GL]^+$ and $[G^\bullet GI]^+$ because of their high radical migration barriers (45.9 and 45.7 kcal mol^{-1}, respectively).

Mechanisms for the Formation of γ-Carbon-Centered Radicals at the (Iso)Leucine Residues and Their Subsequent 56 Da Losses Through C_α−C_β Bond Cleavages. $[GR(L/I)_\gamma^\bullet]^+$ radical cations can be formed by positioning the side chain of the (iso)leucine residue close to the N-terminal α-radical of $[G^\bullet R(L/I)]^+$ through a series of single-bond rotations followed by a "long-range" 1,9-hydrogen-atom transfer directly from the γ-carbon atom of the (iso)leucine residue to the N-terminal α-carbon atom. The barriers against these direct long-range hydrogen atom transfers via the transition structures $TS[G^\bullet RL]^+ \rightarrow [GRL_\gamma^\bullet]^+$ and $TS[G^\bullet RI]^+ \rightarrow [GRI_\gamma^\bullet]^+$ (Figure 6) are 39.0 and 41.0 kcal mol^{-1}, respectively. Again, these values are lower than those for

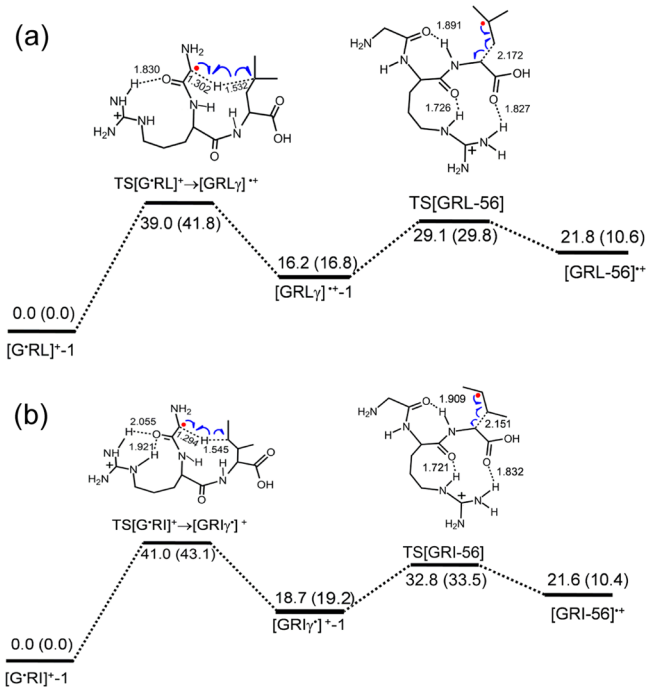

Figure 6. PES for the side cleavage of (a) $[G^\bullet RL]^+$(56 loss) and (b) $[G^\bullet RI]^+$ (56 loss). The radicals as shown in the transition structures of the side cleavage indicate their original location in the corresponding reactants. The enthalpies at 0 K and free energies at 298 K (in parentheses) are shown in kcal mol^{-1}. Selected bond lengths are in Å.

the nonarginyl-containing analogs (by 10.1 and 8.3 kcal mol^{-1}, respectively) and are comparable with the energy barriers against the radical migrations along the backbone (36−39 kcal mol^{-1}; summarized in Scheme S2 of the Supporting Information). The hydrogen bond formed between the guanidino group and the first amide oxygen atom helped to stabilize the transition structures. A less-favorable mechanism for GRL involves a series of stepwise radical migrations: from the N-terminal α-carbon atom to the α-carbon atom of the arginine residue and then to the leucine side-chain γ-carbon atom; the barrier for this mechanism is 43.8 kcal mol^{-1} (4.8 kcal mol^{-1} higher than that for the direct pathway; see Figure S4 of the Supporting Information).

With regard to the C_β−C_γ bond cleavage of the (iso)leucine residue in the α-radical of $[GRL^\bullet]^+$ or $[GRI^\bullet]^+$, the loss of 56 Da (as butane or isobutene, respectively) follows a simple homolytic cleavage of the C_α−C_β bond via a transition structure ((TS[GRL-56] (Figure 6a) or TS[GRI-56] (Figure 6b)) that is very similar to the local minimal structure ($[GRL_\gamma^\bullet]^+$-1 or $[GRI_\gamma^\bullet]^+$-1, respectively). The barriers against the C_α−C_β bond cleavages of $[GRL_\gamma^\bullet]^+$-1 and $[GRI_\gamma^\bullet]^+$-1 are 12.9 and 14.1 kcal mol^{-1}, respectively (or 29.1 and 32.8 kcal mol^{-1}, respectively, relative to their lowest-energy isomers, $[G^\bullet RL]^+$-1 and $[G^\bullet RI]^+$-1, respectively). Once again, we attribute the barrier for GRL being lower than that for GRI to the leucine side chain being larger than the isoleucine side chain, resulting in the C_α−C_β bond of the leucine residue in $[GRL_\gamma^\bullet]^+$-1 (1.561 Å, Figure 3d) being longer than that (1.556 Å, Figure S1d of the Supporting Information) of the isoleucine residue in $[GRI_\gamma^\bullet]^+$-1. Both of these barriers are much lower than those for the corresponding hydrogen atom transfers leading to the formation of the precursors $[GRL_\gamma^\bullet]^+$-1 (39.0 kcal mol^{-1}) and $[GRI_\gamma^\bullet]^+$-1 (41.0 kcal mol^{-1}), suggesting that the rates of

dx.doi.org/10.1021/jp301882p | J. Phys. Chem. B 2012, 116, 7627−7634

the side-chain $C_\alpha-C_\beta$ bond cleavages of $[G^\bullet R(L/I)]^+$ species are also determined by the barriers against the radical migrations.

CONCLUSIONS

CIDs of the two isomeric radical cationic tripeptides $[G^\bullet GL]^+$ and $[G^\bullet GI]^+$, with well-defined initial radical sites at their first α-carbon atoms, generate $[b_2 - H]^{\bullet+}$ species as the predominant ions. Replacing the middle glycine residue with an arginine residue, giving $[G^\bullet RL]^+$ and $[G^\bullet RI]^+$, respectively, leads to the formation of a rich array of fragment ions (a_2^+, $[a_3 + H]^{\bullet+}$, $[b_2 - H]^{\bullet+}$, $[c_2 + 2H]^+$, y_2^+, $[M - 56]^{\bullet+}$) and some diagnostic ions resulting from side chain losses ($[GRL - 43]^+$, $[GRL - 44 - 43]^+$, $[GRI - 29]^+$, $[GRI - 44 - 29]^+$). The distinct differences in the fragmentations of the arginyl- and nonarginyl-containing peptide radical ions reveal that the radicals migrate more readily in the presence of the basic arginine residue. This finding is supported by DFT calculations, which revealed that the arginine residue sequesters the mobile proton, resulting in (i) higher energy barriers against the charge-driven pathways and (ii) energy barriers for hydrogen atom transfers in $[G^\bullet R(L/I)]^+$ that are lower (by 6.9−8.1 kcal mol^{-1}) than those in $[G^\bullet G(L/I)]^+$, thereby allowing the formation of α-carbon-centered radicals at the (iso)leucine residues to initiate the corresponding $C_\beta-C_\gamma$ side chain cleavages. We obtained evidence for this feature experimentally by observing the CID behavior of $[G^\bullet RL_{\alpha\text{-Me}}]^+$, which cannot form an α-carbon-centered radical at the leucine residue and, thereby, inhibits the diagnostic loss of 43 Da from the leucine residue. Similarly, the energy barrier against the radical migration from the α- to the γ-carbon atom of the (iso)leucine side chain via direct hydrogen atom transfer was also substantially lowered (by ~10 kcal mol^{-1}, compared with the nonarginine-containing analogues), facilitating subsequent γ-radical-initiated $C_\alpha-C_\beta$ bond cleavage.

ASSOCIATED CONTENT

Supporting Information

Optimized lowest-energy structures for $[G^\bullet RI]^+$, $[GR^\bullet I]^+$, $[GRI^\bullet]^+$, and $[GRL_\gamma^\bullet]^+$; potential energy surface for radical migration of GRL, GGL radical cation; possible pathways for the formation of $[b_2 - H]^{\bullet+}$ ion from $[G^\bullet RL]^+$; isomerizations and dissociations pathways of $[G^\bullet G(I/L)]^+$, $[G^\bullet R(I/L)]^+$; Cartesian coordinates and vibrational frequencies for the involved stationary points. This information is available free of charge via the Internet at http://pubs.acs.org.

AUTHOR INFORMATION

Corresponding Author

*E-mail: (I.K.C.) ivankchu@hku.hk; (C.-K.S.) chiksiu@cityu.edu.hk.

Author Contributions

§These authors contributed equally to this work.

Notes

The authors declare no competing financial interest.

ACKNOWLEDGMENTS

This study was supported by the Hong Kong Research Grants Council (RGC), Hong Kong Special Administrative Region, China (Project Nos. HKU7016/10P and HKU7016/11P). D.C.M.N., T.S., and Q.Q. thank the Hong Kong RGC for supporting their studentships. C.K.S. thanks the RGC and the City University of Hong Kong (Project No. CityU 103110) for financial support.

REFERENCES

(1) Aebersold, R.; Mann, M. *Nature* **2003**, *422*, 198−207.
(2) Zubarev, R. A.; Horn, D. M.; Fridriksson, E. K.; Kelleher, N. L.; Kruger, N. A.; Lewis, M. A.; Carpenter, B. K.; McLafferty, F. W. *Anal. Chem.* **2000**, *72*, 563−573.
(3) Syka, J. E. P.; Coon, J. J.; Schroeder, M. J.; Shabanowitz, J.; Hunt, D. F. *Proc. Natl. Acad. Sci. U.S.A.* **2004**, *101*, 9528−9533.
(4) Zubarev, R. A. *Curr. Opin. Biotechnol.* **2004**, *15*, 12−16.
(5) Han, H. L.; Xia, Y.; McLuckey, S. A. *J. Proteome Res.* **2007**, *6*, 3062−3069.
(6) Sargaeva, N. P.; Lin, C.; O'Connor, P. B. *Anal. Chem.* **2009**, *81*, 9778−9786.
(7) Levis, R. J. *Annu. Rev. Phys. Chem.* **1994**, *45*, 483−518.
(8) Frank, A. J.; Tureček, F. *J. Phys. Chem. A* **1999**, *103*, 5348−5361.
(9) Barlow, C. K.; McFadyen, W. D.; O'Hair, R. A. J. *J. Am. Chem. Soc.* **2005**, *127*, 6109−6115.
(10) Hodyss, R.; Cox, H. A.; Beauchamp, J. L. *J. Am. Chem. Soc.* **2005**, *127*, 12436−12437.
(11) Hopkinson, A. C.; Siu, K. W. M. Peptide Radical Cations. In *Principles of Mass Spectrometry Applied to Biomolecules*; Laskin, J., Lifshitz, C., Eds.; Wiley Interscience: New York, 2006; pp 301−335.
(12) Matsumoto, Y.; Watanabe, K. *Chem. Rev.* **2006**, *106*, 4234−4260.
(13) Laskin, J.; Yang, Z. B.; Lam, C.; Chu, I. K. *Anal. Chem.* **2007**, *79*, 6607−6614.
(14) Ly, T.; Julian, R. R. *J. Am. Chem. Soc.* **2008**, *130*, 351−358.
(15) Ly, T.; Julian, R. R. *Angew. Chem., Int. Ed.* **2009**, *48*, 7130−7137.
(16) Zhang, L. Y.; Reilly, J. P. *J. Am. Soc. Mass Spectrom.* **2009**, *20*, 1378−1390.
(17) Hopkinson, A. C. *Mass Spectrom. Rev.* **2009**, *28*, 655−671.
(18) Rauk, A.; Yu, D.; Armstrong, D. A. *J. Am. Chem. Soc.* **1997**, *119*, 208−217.
(19) Rauk, A.; Yu, D.; Taylor, J.; Shustov, G. V.; Block, D. A.; Armstrong, D. A. *Biochemistry* **1999**, *38*, 9089−9096.
(20) Tureček, F.; Carpenter, F. H. *J. Chem. Soc., Perkin Trans. 2* **1999**, 2315−2323.
(21) Tureček, F.; Carpenter, F. H.; Polce, M. J.; Wesdemiotis, C. *J. Am. Chem. Soc.* **1999**, *121*, 7955−7956.
(22) Chu, I. K.; Rodriquez, C. F.; Lau, T. C.; Hopkinson, A. C.; Siu, K. W. M. *J. Phys. Chem. B* **2000**, *104*, 3393−3397.
(23) Polce, M. J.; Wesdemiotis, C. *J. Mass Spectrom.* **2000**, *35*, 251−257.
(24) Simon, S.; Sodupe, M.; Bertrán, J. *J. Phys. Chem. A* **2002**, *106*, 5697.
(25) Wee, S.; O'Hair, R. A. J.; McFadyen, W. D. *Rapid Commun. Mass Spectrom.* **2002**, *16*, 5697−5702.
(26) Leymarie, N.; Costello, C. E.; O'Connor, P. B. *J. Am. Chem. Soc.* **2003**, *125*, 8949−8958.
(27) Bagheri-Majdi, E.; Ke, Y. Y.; Orlova, G.; Chu, I. K.; Hopkinson, A. C.; Siu, K. W. M. *J. Phys. Chem. B* **2004**, *108*, 11170−11181.
(28) Wee, S.; O'Hair, R. A. J.; McFadyen, W. D. *Int. J. Mass Spectrom.* **2004**, *234*, 101−122.
(29) Simon, S.; Gil, A.; Sodupe, M.; Bertrán, J. *J. Mol. Struct.: THEOCHEM* **2005**, *727*, 191−197.
(30) Moran, D.; Jacob, R.; Wood, G. P. F.; Coote, M. L.; Davies, M. J.; O'Hair, R. A. J.; Easton, C. J.; Radom, L. *Helv. Chim. Acta* **2006**, *89*, 2254−2272.
(31) O'Connor, P. B.; Lin, C.; Cournoyer, J. J.; Pittman, J. L.; Belyayev, M.; Budnik, B. A. *J. Am. Soc. Mass Spectrom.* **2006**, *17*, 576−585.
(32) Laskin, J.; Futrell, J. H.; Chu, I. K. *J. Am. Chem. Soc.* **2007**, *129*, 9598−9599.
(33) Menon, A. S.; Wood, G. P. F.; Moran, D.; Radom, L. *J. Phys. Chem. A* **2007**, *111*, 13638−13644.
(34) Gil, A.; Simon, S.; Sodupe, M.; Bertrán, J. *Chem. Phys. Lett.* **2008**, *451*, 276−281.

(35) Hayakawa, S.; Matsubara, H.; Panja, S.; Hvelplund, P.; Nielsen, S. B.; Chen, X. H.; Tureček, F. *J. Am. Chem. Soc.* **2008**, *130*, 7645−7654.
(36) Siu, C. K.; Ke, Y.; Guo, Y.; Hopkinson, A. C.; Siu, K. W. M. *Phys. Chem. Chem. Phys.* **2008**, *10*, 5908−5918.
(37) Siu, C. K.; Ke, Y.; Orlova, G.; Hopkinson, A. C.; Siu, K. W. M. *J. Am. Soc. Mass Spectrom.* **2008**, *19*, 1799−1807.
(38) Steill, J.; Zhao, J.; Siu, C.; Ke, Y.; Verkerk, U. H.; Oomens, J.; Dunbar, R. C.; Hopkinson, A. C.; Siu, K. W. M. *Angew. Chem., Int. Ed.* **2008**, *47*, 9666−9668.
(39) Tureček, F.; Jones, J. W.; Towle, T.; Panja, S.; Nielsen, S. B.; Hvelplund, P.; Paizs, B. *J. Am. Chem. Soc.* **2008**, *130*, 14584−14596.
(40) Wood, G. P. F.; Gordon, M. S.; Radom, L.; Smith, D. M. *J. Chem. Theory Comput.* **2008**, *4*, 1788−1794.
(41) Yang, Z. B.; Lam, C.; Chu, I. K.; Laskin, J. *J. Phys. Chem. B* **2008**, *112*, 12468−12478.
(42) Ryzhov, V.; Lam, A. K. Y.; O'Hair, R. A. J. *J. Am. Soc. Mass Spectrom.* **2009**, *20*, 985−995.
(43) Sun, Q. Y.; Nelson, H.; Ly, T.; Stoltz, B. M.; Julian, R. R. *J. Proteome Res.* **2009**, *8*, 958−966.
(44) Jones, J. L.; Dongré, A. R.; Somogyi, Á.; Wysocki, V. H. *J. Am. Chem. Soc.* **1994**, *116*, 8368−8369.
(45) Dongré, A. R.; Jones, J. L.; Somogyi, Á.; Wysocki, V. H. *J. Am. Chem. Soc.* **1996**, *118*, 8365−8374.
(46) Tsaprailis, G.; Nair, H.; Somogyi, Á.; Wysocki, V. H.; Zhong, W.; Futrell, J. H.; Summerfield, S. G.; Gaskell, S. J. *J. Am. Chem. Soc.* **1999**, *121*, 5142−5154.
(47) Wysocki, V. H.; Tsaprailis, G.; Smith, L. L.; Breci, L. A. *J. Mass Spectrom.* **2000**, *35*, 1399−1406.
(48) Chung, T.; Tureček, F. *J. Am. Soc. Mass Spectrom.* **2010**, *21*, 1279−1295.
(49) Moore, B. N.; Ly, T.; Julian, R. R. *J. Am. Chem. Soc.* **2011**, *133*, 6997−7006.
(50) Bythell, B.; Hendrickson, C.; Marshall, A. *J. Am. Soc. Mass Spectrom.* **2012**, *23*, 644−654.
(51) Chu, I. K.; Zhao, J.; Xu, M.; Siu, S. O.; Hopkinson, A. C.; Siu, K. W. M. *J. Am. Chem. Soc.* **2008**, *130*, 7862−7872.
(52) Ng, D. C. M.; Song, T.; Siu, S. O.; Siu, C. K.; Laskin, J.; Chu, I. K. *J. Phys. Chem. B* **2010**, *114*, 2270−2280.
(53) Siu, C. K.; Zhao, J. F.; Laskin, J.; Chu, I. K.; Hopkinson, A. C.; Siu, K. W. M. *J. Am. Soc. Mass Spectrom.* **2009**, *20*, 996−1005.
(54) Song, T.; Ng, D. C. M.; Quan, Q.; Siu, C.-K.; Chu, I. K. *Chem.—Asian J.* **2011**, *6*, 888−898.
(55) Wee, S.; Mortimer, A.; Moran, D.; Wright, A.; Barlow, C. K.; O'Hair, R. A. J.; Radom, L.; Easton, C. J. *Chem. Commun.* **2006**, 4233−4235.
(56) Pingitore, F.; Bleiholder, C.; Paizs, B.; Wesdemiotis, C. *Int. J. Mass Spectrom.* **2007**, *265*, 251−260.
(57) Henke, W.; Kremer, S.; Reinen, D. *Inorg. Chem.* **1983**, *22*, 2858−2863.
(58) Varkey, S. P.; Ratnasamy, C.; Ratnasamy, P. *J. Mol. Catal. A: Chem* **1998**, *135*, 295−306.
(59) Chan, W. C.; White, P. D. *FMOC Solid Phase Peptide Synthesis: A Practical Approach*; Oxford University Press: New York, 2000.
(60) *SPARTAN, '04 Essential V2.0.0*; Wavefunction, Inc.: Irvine, CA, 2004.
(61) Becke, A. D. *Chem. Phys.* **1993**, *98*, 5648−5652.
(62) Frisch, M. J.; Trucks, G. W.; Schlegel, H. B.; Scuseria, G. E.; Robb, M. A.; Cheeseman, J. R.; Montgomery, J. A., Jr.; Vreven, T.; Kudin, K. N.; Burant, J. C.; Millam, J. M.; Iyengar, S. S.; Tomasi, J.; Barone, V.; Mennucci, B.; Cossi, M.; Scalmani, G.; Rega, N.; Petersson, G. A.; Nakatsuji, H.; Hada, M.; Ehara, M.; Toyota, K.; Fukuda, R.; Hasegawa, J.; Ishida, M.; Nakajima, T.; Honda, Y.; Kitao, O.; Nakai, H.; Klene, M.; Li, X.; Knox, J. E.; Hratchian, H. P.; Cross, J. B.; Bakken, V.; Adamo, C.; Jaramillo, J.; Gomperts, R.; Stratmann, R. E.; Yazyev, O.; Austin, A. J.; Cammi, R.; Pomelli, C.; Ochterski, J. W.; Ayala, P. Y.; Morokuma, K.; Voth, G. A.; Salvador, P.; Dannenberg, J. J.; Zakrzewski, V. G.; Dapprich, S.; Daniels, A. D.; Strain, M. C.; Farkas, O.; Malick, D. K.; Rabuck, A. D.; Raghavachari, K.; Foresman, J. B.; Ortiz, J. V.; Cui, Q.; Baboul, A. G.; Clifford, S.; Cioslowski, J.; Stefanov, B. B.; Liu, G.; Liashenko, A.; Piskorz, P.; Komaromi, I.; Martin, R. L.; Fox, D. J.; Keith, T.; Al-Laham, M. A.; Peng, C. Y.; Nanayakkara, A.; Challacombe, M.; Gill, P. M. W.; Johnson, B.; Chen, W.; Wong, M. W.; Gonzalez, C.; Pople, J. A. *Gaussian 03, Revision C.02*; Gaussian, Inc.: Wallingford, CT, 2004.
(63) Hehre, W. J.; Ditchfield, R.; Pople, J. A. *J. Chem. Phys.* **1972**, *56*, 2257.
(64) Clark, T.; Chandrasekhar, J.; Spitznagel, G. W.; Schleyer, P. v. R. *J. Comput. Chem.* **1983**, *4*, 294−301.
(65) Xu, M.; Song, T.; Quan, Q.; Hao, Q.; Fang, D. C.; Siu, C. K.; Chu, I. K. *Phys. Chem. Chem. Phys.* **2011**, *13*, 5888−5896.
(66) Laskin, J.; Yang, Z.; Ng, C. M. D.; Chu, I. K. *J. Am. Soc. Mass Spectrom.* **2010**, *21*, 511−521.
(67) Chu, I. K.; Siu, S. O.; Lam, C. N. W.; Chan, J. C. Y.; Rodriquez, C. F. *Rapid Commun. Mass Spectrom.* **2004**, *18*, 1798−1802.
(68) Schnier, P. D.; Price, W. D.; Jockusch, R. A.; Williams, E. R. *J. Am. Chem. Soc.* **1996**, *118*, 7178−7189.
(69) Harrison, A.; Csizmadia, I.; Tang, T.-H. *J. Am. Soc. Mass Spectrom.* **2000**, *11*, 427−436.
(70) Farrugia, J. M.; O'Hair, R. A. J. *Int. J. Mass Spectrom.* **2003**, *222*, 229−242.
(71) Bythell, B. J.; Suhai, S.; Somogyi, Á.; Paizs, B. *J. Am. Chem. Soc.* **2009**, *131*, 14057−14065.
(72) Bythell, B. J.; Csonka, I. P.; Suhai, S.; Barofsky, D. F.; Paizs, B. *J. Phys. Chem. B* **2010**, *114*, 15092−15105.
(73) Zhao, J.; Song, T.; Xu, M.; Quan, Q.; Siu, K. W. M.; Hopkinson, A. C.; Chu, I. K. *Phys. Chem. Chem. Phys.* **2012**, *14*, 8723−8731.